J|A|C|S ARTICLES

Published on Web 12/08/2010

Delivery and Subcellular Targeting of Dendrimer-Based Fluorescent pH Sensors in Living Cells

Lorenzo Albertazzi,*[,†,‡] Barbara Storti,[†,‡] Laura Marchetti,[†] and Fabio Beltram[†,‡]

NEST, Scuola Normale Superiore and Istituto Nanoscienze-CNR and IIT@NEST, Center for Nanotechnology Innovation, 56127 Pisa, Italy

Received July 8, 2010; E-mail: l.albertazzi@sns.it

Abstract: Synthesis and targeted delivery of dendrimer-based fluorescent biosensors in living HeLa cells are reported. Following electroporation dendrimers are shown to display specific subcellular localization depending on their size and surface charge and this property is preserved when they are functionalized with sensing moieties. We analyze the case of double dendrimer conjugation with pH-sensitive and pH-insensitive molecules leading to the realization of ratiometric pH sensors that are calibrated *in vitro* and in living cells. By tuning the physicochemical properties of the dendrimer scaffold sensors can be targeted to specific cellular compartments allowing selective pH measurements in different organelles in living cells. In order to demonstrate the modularity of this approach we present three different pH sensors with tuned H^+ affinity by appropriately choosing the pH-sensitive dye. We argue that the present methodology represents a general approach toward the realization of targetable ratiometric sensors suitable to monitor biologically relevant ions or molecules in living cells.

Introduction

Dendrimers are very promising tools for biomedical purposes.[1] Their unique treelike structure endows them with many attractive properties such as monodispersity, biocompatibility, and tunable chemical properties.[2] In particular, they were successfully employed for a wide range of applications such as drug[3] or gene[4] delivery and as contrast agents.[5]

Recent pioneering works employed dendrimers as scaffolds for the realization of biosensors. Colorimetric,[6] electrochemical,[7] and fluorescent[8] sensors were developed by exploiting the physicochemical properties of dendrimers. This approach seems to be particularly promising for in vivo measurements of biologically relevant analytes thanks to its potentially high biocompatibility, as recently demonstrated by in vivo oxygen imaging performed by Vinogradov and co-workers.[9] Application of these sensors to the biological environment and in particular to live cells is, however, still very limited. This likely stems from difficulties in sensor delivery and from the poor understanding of dendrimer behavior in living cells.

Two main families of fluorescent sensors are currently investigated in the literature: fluorescent proteins (FP)-based sensors and small organic dyes with an analyte-dependent luminescence. FP sensors are extensively used thanks to their easy cellular delivery and targeting and for their high biocompatibility.[10,11] Their range of application, however, is reduced owing to the restricted range of ions or molecules that they can sense. On the other hand, there is a very large range of small organic fluorophores successfully employed to measure biologically relevant ions (such as calcium,[12] sodium,[13]

* To whom correspondence should be addressed. .
† NEST, Scuola Normale Superiore and Istituto Nanoscienze-CNR.
‡ IIT@NEST, Center for Nanotechnology Innovation.

(1) (a) Lee, C. C.; MacKay, J. A.; Frechet, J. M.; Szoka, F. C. *Nat. Biotechnol.* **2005**, *23*, 1517–26. (b) Tekade, R. K.; Kumar, P. V.; Jain, N. K. *Chem. Rev.* **2009**, *109*, 49–87. (c) Astruc, D.; Boisselier, E.; Ornelas, C. *Chem. Rev.* **2010**, *110*, 1857. (d) Rolland, O.; Turrin, C. O.; Caminade, A. M.; Majoral, J. P. *New J. Chem.* **2009**, *33*, 1809.

(2) (a) Tomalia, D. A.; Huang, B.; Swanson, D. R.; Brothers, H. M.; Klimash, J. W. *Tetrahedron* **2003**, *59*, 3799–3813. (b) Gillies, E. R.; Dy, E.; Frechet, J. M.; Szoka, F. C. *Mol. Pharm.* **2005**, *2*, 129–38. (c) Lim, J.; Simanek, E. E. *Mol. Pharm.* **2005**, *2*, 273–7. (d) Kang, T.; Amir, R. J.; Khan, A.; Ohshimizu, K.; Hunt, J. N.; Sivanandan, K.; Montanez, M. I.; Malkoch, M.; Ueda, M.; Hawker, C. J. *Chem. Commun. (Cambridge, U.K.)* **2010**, *46*, 1556–8.

(3) (a) Lee, C. C.; Gillies, E. R.; Fox, M. E.; Guillaudeu, S. J.; Frechet, J. M.; Dy, E. E.; Szoka, F. C. *Proc. Natl. Acad. Sci. U.S.A.* **2006**, *103*, 16649–54. (b) Majoros, I. J.; Myc, A.; Thomas, T.; Mehta, C. B.; Baker, J. R., Jr. *Biomacromolecules* **2006**, *7*, 572–9.

(4) (a) Caminade, A. M.; Turrin, C. O.; Majoral, J. P. *Chemistry* **2008**, *14*, 7422–32. (b) Zhou, J.; Wu, J.; Hafdi, N.; Behr, J. P.; Erbacher, P.; Peng, L. *Chem. Commun. (Cambridge, U.K.)* **2006**, *22*, 2362–4. (c) Mintzer, M. A.; Simanek, E. E. *Chem. Rev.* **2009**, *109*, 259–302.

(5) (a) Xu, H.; Regino, C. A.; Koyama, Y.; Hama, Y.; Gunn, A. J.; Bernardo, M.; Kobayashi, H.; Choyke, P. L.; Brechbiel, M. W. *Bioconjug. Chem.* **2007**, *18*, 1474–82. (b) Kobayashi, H.; Koyama, Y.; Barrett, T.; Hama, Y.; Regino, C. A.; Shin, I. S.; Jang, B. S.; Le, N.; Paik, C. H.; Choyke, P. L.; Urano, Y. *ACS Nano* **2007**, *1*, 258–64.

(6) Rakow, N. A.; Suslick, K. S. *Nature* **2000**, *406*, 710–3.

(7) Armada, M. P.; Losada, J.; Zamora, M.; Alonso, B.; Cuadrado, I.; Casado, C. M. *Bioelectrochemistry* **2006**, *69*, 65–73.

(8) (a) Finikova, O.; Galkin, A.; Rozhkov, V.; Cordero, M.; Hagerhall, C.; Vinogradov, S. *J. Am. Chem. Soc.* **2003**, *125*, 4882–93. (b) Balzani, V.; Ceroni, P., Gestermann, S.; Kauffmann, C.; Gorka, C.; Vogtle, F. *Chem. Commun. (Cambridge, U.K.)* **2000**, 853–854.

(9) (a) Lebedev, A. Y.; Cheprakov, A. V.; Sakadzic, S.; Boas, D. A.; Wilson, D. F.; Vinogradov, S. A. *ACS Appl. Mater. Interfaces* **2009**, *1*, 1292–1304. (b) Wilson, D. F.; Lee, W. M.; Makonnen, S.; Apreleva, S.; Vinogradov, S. A. *Adv. Exp. Med. Biol.* **2008**, *614*, 53–62.

(10) Palmer, A. E.; Tsien, R. Y. *Nat. Protoc.* **2006**, *1*, 1057–65.

(11) Bizzarri, R.; Arcangeli, C.; Arosio, D.; Ricci, F.; Faraci, P.; Cardarelli, F.; Beltram, F. *Biophys. J.* **2006**, *90*, 3300–14.

(12) Ren, Y.; Ridsdale, A.; Coderre, E.; Stys, P. K. *J. Neurosci. Methods* **2000**, *102*, 165–76.

(13) Rose, C. R.; Konnerth, A. *J. Neurosci.* **2001**, *21*, 4207–14.

10.1021/ja105689u

potassium,[14,15] zinc[16]), pH,[17] small molecules,[18] and even physical parameters such as membrane potential[19] and polarity.[20] Although these molecules can be exploited to monitor many important analytes, they also present the following limitations: (i) it is difficult to target them to specific cellular compartments; (ii) they often do not allow ratiometric imaging so that it is not possible to achieve absolute, quantitative measurements; (iii) many indicators suffer from poor solubility in water and consequently display poor biocompatibility; and (iv) some indicators show cell leakage and limit the span of time-lapse imaging.[21]

The objective of the present article is two-fold. (i) We present a methodology to efficiently deliver fluorescent dendrimers into living cells to specific intracellular compartment; and ii) we realize dendrimer-based ratiometric pH sensors that overcome several of the limitations characteristic of organic probes.

Fluorescently labeled dendrimers were delivered into living cells by electroporation and their different size (from G2 up to G6) and surface charge (cationic and neutral) were exploited to target dendrimer-based sensors to specific cell compartments.

Ratiometric pH sensors were synthesized and studied in vitro and in live HeLa cells, yielding in the latter case targeted pH maps with high spatial and temporal resolution.

We exploited the modularity of this approach to realize three different pH sensors with tuned H^+ affinity. Importantly, the synthetic procedure shown here can be used for other sensing dyes so that the sensors presented here actually represent a model for a family of dendrimer-based sensors of interest for other biologically relevant ions and small molecules.

Materials and Methods

Materials. G2, G4, G6 PAMAM dendrimers, acetic anhydride, Fluorescein, and Amicon ultra 10 KDa dyalisis membranes were purchased from SigmaAldrich. Alexa 647 dye, Oregon Green, Rhodamine Red, lysosensor, DAPI, Syto81, and DiI were purchased from Invitrogen. NMR spectra were acquired by means of a Varian 300 MHz spectrometer. IR spetra were obtained with a Perkin-Elmer FT-IR instrument.

General Procedure for PAMAM Dendrimer Acetylation. Synthesis and characterization of aceylated dendrimers were extensively described elsewhere.[22,23]

Briefly, ethylenediamine core PAMAM dendrimers were dissolved in anhydrous methanol with triethylamine and an excess of acetic anhydride, and the solution was stirred overnight at room temperature. The product was diluted with deionized water and extensively dialyzed against water (molecular weight cutoff (MWCO) = 10 KDa) to afford the acetylated dendrimer. Dendrimer acetylation was verified by means of NMR spectroscopy.

General Procedure for Fluorophore Labeling of PAMAM Dendrimers. Dendrimer-fluorophore conjugation was carried out via amide bonding between the primary amine of the dendrimer and the *N*-hydroxysuccinimide-activated carboxyl of the fluorophores. Dendrimers were dissolved in DMSO and the reactive dye was added. The solution was stirred for 12 h at room temperature, diluted with water, and then dialyzed against water (MWCO = 10 KDa) to afford dendrimer-dye conjugates. A full characterization of dye-labeled PAMAM dendrimers used in this work was recently reported.[23]

UV−vis Spectrofluorimetry. Excitation and emission spectra were recorded by means of a Cary Eclipse fluorometer (Varian, Palo Alto, CA).Typically, 500 μL samples were used in a quartz cuvette (Hellma, Milan, Italy). The temperature of the cell compartment was controlled by a built-in Peltier cooler (Varian). Excitation and emission band-pass of 5 nm was employed.

Dynamic Light Scattering (DLS). Size measurements of labeled PAMAM dendrimers were achieved by means of a Zetasizer Nano ZS90 (Malvern Instruments). Measurements were performed using a He−Ne 633 nm laser keeping the cell compartment temperature constant at 25 °C.

Cell Culture and Electroporation. HeLa and CHO cell lines were purchased from ATCC and cultured following manufacturer's instructions. For live-cell, microscopy cells were plated onto 35 mm glass-bottom dishes (WillCo-dish GWSt-3522) and imaged at 37 °C, 5% CO_2. Electroporation was performed using Microporator (Digital Bio Technology, Korea) according to manufacturer instructions for HeLa cultures. Cells were resuspended in microporation buffer (Digital Bio Technology) containing dendrimers (250 nM and 2 μM for cationic and neutral PAMAM, respectively). Electroporation was performed with 10 μL volume-sized tip for neutral dendrimer and 100 μL volume-sized tip for charged dendrimers. In the case of charged dendrimers, after electroporation cells were centrifuged for 5 min at 1200 rpm to remove the excess of dendrimer in the medium. Cells were washed and fresh medium was added before imaging, usually 12−18 h after electroporation.

Confocal Imaging. Cell imaging was performed with a Leica TCS SP2 inverted confocal microscope (Leica Microsystems) equipped with a 40× 1.25 NA oil immersion objective (Leica Microsystems). Imaging was obtained illuminating the samples with the Ar and He−Ne lasers and with a 403 nm pulsed diode laser (M8903−01; Hamamatsu) at 50 MHz repetition rate. Fluorescence emission was collected with the microscope AOBS-based built-in detectors.

Preparation of Cytoplasm-Cell Extracts. U2OS cells (ATCC: HTB96) were grown in DMEM, supplemented with 2 mM glutamine, 1 mM sodium pyruvate, 10 U/L penicillin, 10 μg/L streptomycin, and 10% fetal bovine serum (Gibco). Typically 3−5 $\times 10^7$ cells were used for cytoplasm extraction; these were harvested by trypsinization, counted, and washed twice with ice-cold PBS. Similar to what was already reported[24] cytoplasm was extracted resuspending cells (at 4×10^7 cells/mL) in ice cold 15 mM Tris-HCl pH 7.5, 10 mM KCl, 10 mM NaCl, 5 mM $MgCl_2$, 1 mM $CaCl_2$, 300 mM sucrose, 10% glycerol, and 0.1% Triton-X100 for 7 min. This buffer was supplemented with protease inhibitors (leupeptin, aprotinin, PMSF), phosphatase inhibitors (NaF, sodium orthovanadate), 1 mM DTT, and 1 mM ATP prior to use. Low-speed centrifugation (1300 g, 5 min, at 4 °C) allowed separating cytoplasm (supernatant) from intact nuclei (pellet). Lysate protein concentration was finally estimated by Bradford assay (Pierce).

Kinetics of Acetylated-Dendrimer Hydrolysis in the Presence of Cytoplasm Cell Extract. After acetylation, dialyzed dendrimer-based pH sensors were incubated with ∼50−100 μg cytoplasm extract, 1:5 diluted in PBS buffer, at 37 °C. As a control,

(14) Namkung, W.; Song, Y.; Mills, A. D.; Padmawar, P.; Finkbeiner, W. E.; Verkman, A. S. *J. Biol. Chem.* **2009**, *284*, 15916–26.
(15) Padmawar, P.; Yao, X.; Bloch, O.; Manley, G. T.; Verkman, A. S. *Nat. Methods* **2005**, *2*, 825–7.
(16) Burdette, S. C.; Walkup, G. K.; Spingler, B.; Tsien, R. Y.; Lippard, S. J. *J. Am. Chem. Soc.* **2001**, *123*, 7831–41.
(17) Han, J.; Burgess, K. *Chem. Rev.* **2010**, *110*, 2709.
(18) Kojima, H.; Urano, Y.; Kikuchi, K.; Higuchi, T.; Hirata, Y.; Nagano, T. *Angew. Chem., Int. Ed.* **1999**, *38*, 3209–3212.
(19) White, R. J.; Reynolds, I. J. *J. Neurosci.* **1996**, *16*, 5688–97.
(20) Signore, G.; Nifosi, R.; Albertazzi, L.; Storti, B.; Bizzarri, R. *J. Am. Chem. Soc.* **2010**, *132*, 1276–1288.
(21) Silver, R. A.; Whitaker, M.; Bolsover, S. R. *Pflugers Arch.* **1992**, *420*, 595–602.
(22) Shi, X.; Lesniak, W.; Islam, M. T.; Muniz, M. C.; Balogh, L. P.; Baker, J. R., Jr. *Colloids Surf., A* **2006**, *272* (1−2), 139–150.
(23) Albertazzi, L.; Serresi, M.; Albanese, A.; Beltram, F. *Mol. Pharm.* **2010**, *7*, 680–8.
(24) Marchetti, L.; Comelli, L.; D'innocenzo, B.; Puzzi, L.; Luin, S.; Arosio, D.; Calvello, M.; Mendoza-Maldonado, R.; Peverali, F.; Trovato, F.; Riva, S.; Biamonti, G.; Abdurashidova, G.; Beltram, F.; Falaschi, A. *Nucleic Acid Res.* 2010.

dendrimers were incubated in the same conditions with the same volume of cytoplasm-extraction buffer. Fluorescence emission spectra of Oregon Green, Fluorescein, and Coumarin were collected at regular time intervals and constant $T = 37$ °C as previously described.

In Vitro Calibration. pH titration of dendrimer-based sensors fluorescence was performed on 1 μM samples dissolved in 2 mM phosphate buffer whose pH was adjusted by small addition of NaOH 0.1 M. Emission spectra of the sensing dye and Rhodamine Red were obtained for each pH. Coumarin, Fluorescein, Oregon Green and Rhodamine Red were excited at 350, 488, 488, and 561 nm, respectively.

Calibration and pH Imaging in HeLa Cells. HeLa cells were electroporated as described above and imaged 12 h after dendrimer administration. Fluorescein and Rhodamine were imaged using the 488 nm (collection from 500 to 550 nm) and the 561 nm (collection from 575 to 700 nm) laser lines of the confocal system, respectively. To obtain a pH, calibration of the sensor cells were clamped at the desired pH by using pH ionophores in a K^+ enriched buffer.[11]

Results

PAMAM Dendrimers-Dye Conjugates. The physicochemical properties of PAMAM dendrimers have been extensively investigated since their early synthesis.[25] In particular amine-terminated and acetylated PAMAMs were studied in much detail and their relevant properties fully characterized by experimental[22,26] and computational techniques.[27] We exploited this information to design dendrimer-based devices where the physicochemical properties of the dendrimer periphery can modulate the interaction with biomolecules within living cells.

To study their intracellular behavior, PAMAM dendrimers varying in size and surface charge were labeled with bright and photostable fluorophores. Amine-terminated PAMAM dendrimers were chosen as a model for cationic dendrimers since primary amines are protonated and bear a positive charge at physiological pH. Generations from G2 up to G6 were chosen to span a broad range of molecular weight and surface charge. To obtain neutral structures, G4 and G6 cationic dendrimers were fully acetylated with acetic anhydride.

Amine-terminated PAMAM dendrimers were labeled with Alexa647 while fully acetylated neutral dendrimer were labeled with Oregon Green 488 (see Figures 1a and 2a, respectively). Neutral dendrimers were labeled before acetylation. By using an excess of acetylating agent, we achieved the acetylation of the free hydroxyl of the fluorophores. This will be relevant for the on/off feature of the pH sensors presented in the next sections.

Electroporation and Intracellular Targeting of Labeled Dendrimers. To study the intracellular behavior of PAMAM dendrimers, we developed a protocol for cell delivery of these macromolecules based on electroporation. Cationic (G2, G4, and G6) and neutral (G4 and G6) fluorescent dendrimers were delivered into living HeLa cells and their intracellular dynamics studied by confocal microscopy. Figure 1a shows the localization of different generations of cationic dendrimers in HeLa cells (Hoechst staining was also used as a nuclear marker). Images show that G2 is homogenously distributed inside cells while G4 and G6 display peculiar localizations. We performed a colocalization assay to reveal which organelles are involved in dendrimers trafficking and the results are reported in Figure 1b. G4 dendrimers colocalize with the syto81 dye, a nucleolar marker.[29] Indeed nucleolar localization was reported also for other cationic molecules able to bind negatively charged RNA.[30] G6 dendrimers instead show a distinct localization pattern and colocalize with a plasma-membrane marker (DiI) and with a lysosome marker (lysotracker).

Figure 2a shows the localization of fully acetylated G4-Ac and G6-Ac dendrimers. Confocal images show that neutral dendrimers show a much less structured localization with respect to their cationic analogs. The only notable aspect is the different distribution between nucleus and cytoplasm for G4 and G6 dendrimers. This can be linked to their different size (G4 14 kDa, G6 58 kDa) as the larger G6 dendrimer cannot freely diffuse from the cytoplasm to the nucleus because it is comparable to the nuclear pore limit.[31]

Some vesicular localization was observed for all dendrimers, probably owing to a small fraction of dendrimer being internalized by endocytosis or compartimentalized after electroporation.

Interestingly, the localization of the neutral G4-Ac is pH dependent, as shown in Figure 2b. Indeed the acidification of the cytoplasm (induced with H^+ ionophores) lead to the accumulation of dendrimers in the nucleoli with a similar localization of the cationic G4 analog: at acidic pH the tertiary amines in the interior of the dendrimers are protonated and therefore the macromolecule can go from neutral to cationic.[32]

These measurements demonstrate that PAMAM dendrimers have structure-dependent specific localization inside cells and therefore intracellular targeting of dendritic structures can be achieved with simple modifications of dendrimer physicochemical properties.

Dendrimer-Based pH Sensors. Multifunctionality, monodispersity, and tunable chemical properties make dendrimers very attractive for the design of biosensors. In this section, we present synthesis and photophysical characterization of three different dendrimer-based pH sensors suitable for in vivo imaging. H^+ ions are relevant in many physiological mechanisms and pH indicators were developed to monitor their intracellular concentration.[17]

Figure 3a schematically shows the synthesis of the sensors. Two different fluorophores were conjugated to the G6 dendritic scaffold: a pH-sensitive dye (carboxyfluorescein in the diagram) and a pH-insensitive rhodamine dye (Rhodamine RedX). Exploiting dendrimer multifunctionality these two moieties can be conjugated to the same macromolecule thus realizing a ratiometric sensor. The pH-sensitive fluorescein signal can be normalized to the pH-independent red signal of rhodamine, thus compensating for the signal-intensity dependence on sensor

(25) (a) Tomalia, D.; Naylor, A.; Goddard, W., III. *Angew. Chem., Int. Ed.* **1990**, *29*, 138–175. (b) Tomalia, D.; Baker, H.; Dewald, J.; Hall, M.; Kallos, G.; Martin, S.; Roeck, J.; Ryder, J.; Smith, P. *Polym. J.* **1985**, *17*, 117–132.
(26) (a) Nourse, A.; Millar, D. B.; Minton, A. P. *Biopolymers* **2000**, *53*, 316–28. (b) Islam, M. T.; Majoros, I. J.; Baker, J. R., Jr. *J. Chromatogr., B: Anal. Technol. Biomed. Life Sci.* **2005**, *822*, 21–6. (c) Majoros, I.; Keszler, B.; Woehler, S.; Bull, T.; Baker, J. R. *Macromolecules* **2003**, *36*, 5526–5529.
(27) (a) Lee, H.; Larson, R. G. *J. Phys. Chem. B* **2006**, *110*, 18204–11.
(28) Pavan, G. M.; Albertazzi, L.; Danani, A. *J. Phys. Chem. B* **2010**, *114*, 2667–75.
(29) Wlodkowic, D.; Skommer, J.; Darzynkiewicz, Z. *Cytometry, Part A* **2008**, *73*, 496–507.
(30) Siomi, H.; Shida, H.; Maki, M.; Hatanaka, M. *J. Virol.* **1990**, *64*, 1803–7.
(31) (a) Cardarelli, F.; Bizzarri, R.; Serresi, M.; Albertazzi, L.; Beltram, F. *J. Biol. Chem.* **2009**, *284*, 36638–46. (b) Cardarelli, F.; Serresi, M.; Bizzarri, R.; Giacca, M.; Beltram, F. *Mol. Ther.* **2007**, *15*, 1313–22.
(32) (a) Cakara, D.; Kleimann, J.; Borkovec, M. *Macromolecules* **2003**, *36*, 4201–4207. (b) Liu, Y.; Bryantsev, V. S.; Diallo, M. S.; Goddard Iii, W. A. *J. Am. Chem. Soc.* **2009**, *131*, 2798–2799.

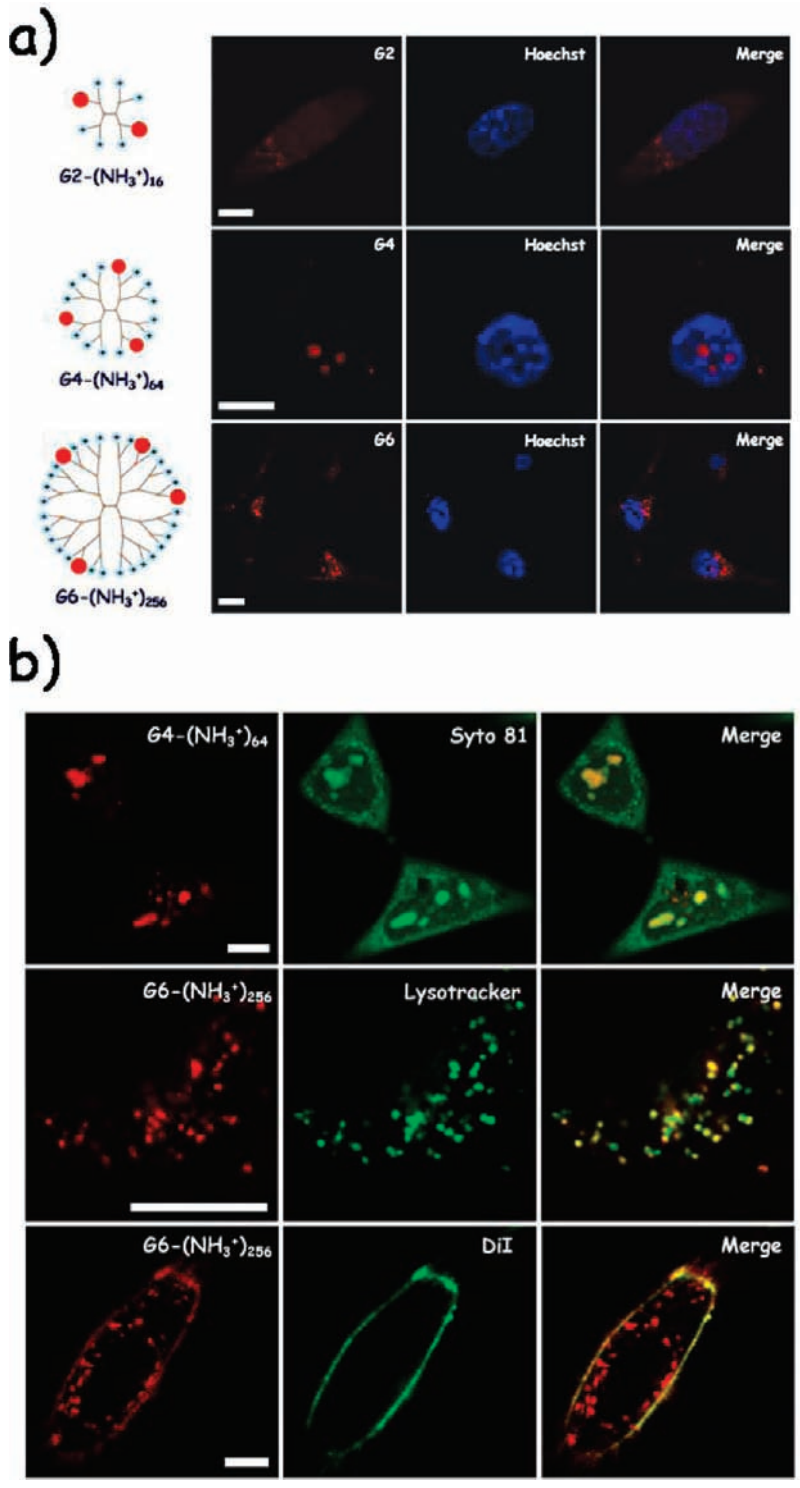

Figure 1. (a) Cationic dendrimers localization after electroporation. Dendrimers varying in size (from G2 up to G6) were studied. Nuclei (in blue) were stained with Hoechst. (b) Colocalization assay for cationic dendrimers (in red) with organelle markers (in green). Scale Bar = 15 μm.

concentration. This is of crucial relevance for the application of the biosensors in vivo.

Figure 3b shows that with the same synthetic approach we realized three different pH sensors based on different commercial dyes: (i) 7-hydroxy-4-methyl-3-coumarinylacetic acid; (ii) 5(6)-carboxyfluorescein; (iii) Oregon Green 488. These three fluorophores are tuned for measurements in alkaline, neutral, and acidic environments, respectively. All conjugates were obtained from the reaction of the *N*-hydroxysuccinimide ester of the dye with the terminal amine of the dendrimer yielding a stable amide bond. The presence of both fluorophores was verified by absorption spectroscopy (see Supporting Information Figure 1).

The cationic dendrimers obtained with this synthetic step can be acetylated to neutralize the surface charge of the sensor using an excess of acetic anhydride. Interestingly, in these conditions the pH-sensitive fluorophores are also acetylated since they all present a free hydroxyl group that is crucial for their fluorescence and sensing properties. Indeed, after

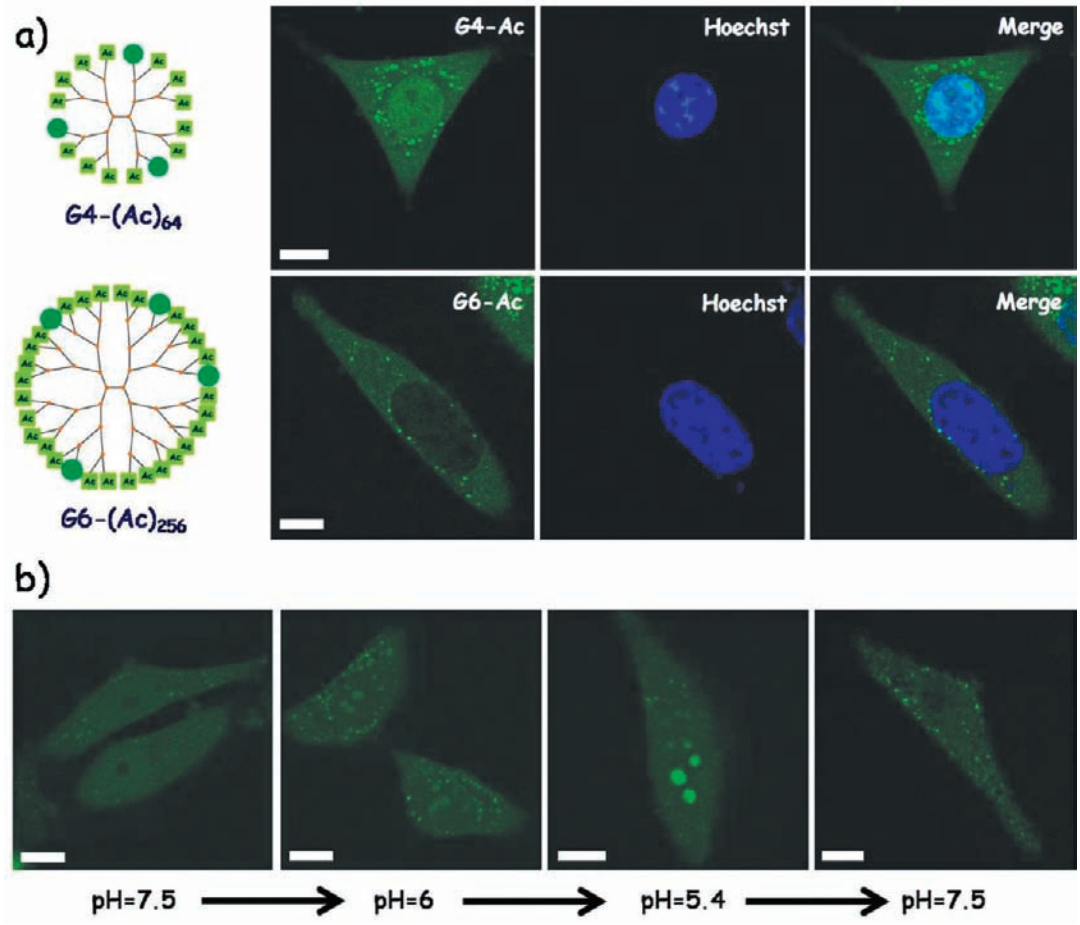

Figure 2. (a) Neutral dendrimers (G4-Ac and G6-Ac) localization after electroporation. Nuclei (in blue) were stained with Hoechst. (b) Representative images of pH-dependent localization of G4-Ac dendrimers. Scale Bar = 15 μm.

acetylation the fluorescence of these molecules is completely quenched while the rhodamine fluorescence is virtually unmodified.

We studied the hydrolysis kinetics of the acetyl esters of the three fluorophores utilized in this work by incubating them with a cytoplasmic cell lysate (i.e., a cell extract of cytoplasmic proteins) to mimic the intracellular conditions of hydrolysis. The recovery of the fluorescence of the pH-sensitive fluorophores induced by the cytoplasmic lysate was compared to the recovery in buffer alone (Figure 3b). All fluorophores show slow fluorescence recovery in buffer that reaches a plateau within about 24 h, while the presence of cytoplasmic enzymes promotes a more rapid hydrolysis kinetics. This difference is considerable for Fluorescein and Oregon Green dyes that display a very fast kinetic in the presence of cell lysate, while it is less marked for the Coumarin dye.

These large differences between in vitro and in living cells conditions can be exploited for the design of cell-activated biosensors that actually turn their fluorescence on only once inside the target cells.

In Vitro Titration. Figure 4 reports in vitro titration data of the pH sensors. Emission spectra of pH-sensitive carboxyfluorescein and rhodamine were recorded at different pH values (Figure 4a). It can be seen that even following excitation at 488 nm a red emission band is present as a consequence of fluorescence resonance energy transfer (FRET); the two molecules are forced in close proximity on the dendrimer structure. Figure 4b reports the fluorescence intensities for the green and the red fluorophores upon pH titration. As expected, fluorescein emission strongly depends on pH while the red fluorophore is virtually pH insensitive in the physiological range ($\Delta F < 10\%$). The ratio between the sensing fluorophores and the rhodamine for the three sensors is reported in Figure 4c. The three titration curves demonstrate that these sensors are suitable to measure pH in different ranges as expected from the H^+ affinities of the dyes employed. Notably some of the photophysical properties of the dyes are not fully retained after dendrimer conjugation. For example, the titration profile of Oregon Green is different from the one reported by the manufacturer for the isolated fluorophore. We observed a similar behavior also with other dendrimer−fluorophore conjugates (data not shown). Although these findings do not affect the ability of the present sensors to yield accurate pH measurements, this aspect deserves further studies.

Calibration and Targeted Intracellular pH Measurements in HeLa Cells. We applied the previously described protocol for electroporation to the dendrimer-based pH sensors. We used the fluorescein-based sensor for living cells studies in light of its ability to measure pH around physiological values; fully acetylated G6-dendrimer sensors were therefore delivered into HeLa cells by electroporation. Figure 5a shows the fluorescence images of dendrimer-treated HeLa cells. Both Fluorescein (green) and rhodamine (red) fluorescence were recorded and ratiometric pH maps were calculated on a pixel-by-pixel basis. To demonstrate the ability of the sensor to measure pH in living cells and to calibrate the sensor, pH was set to different values

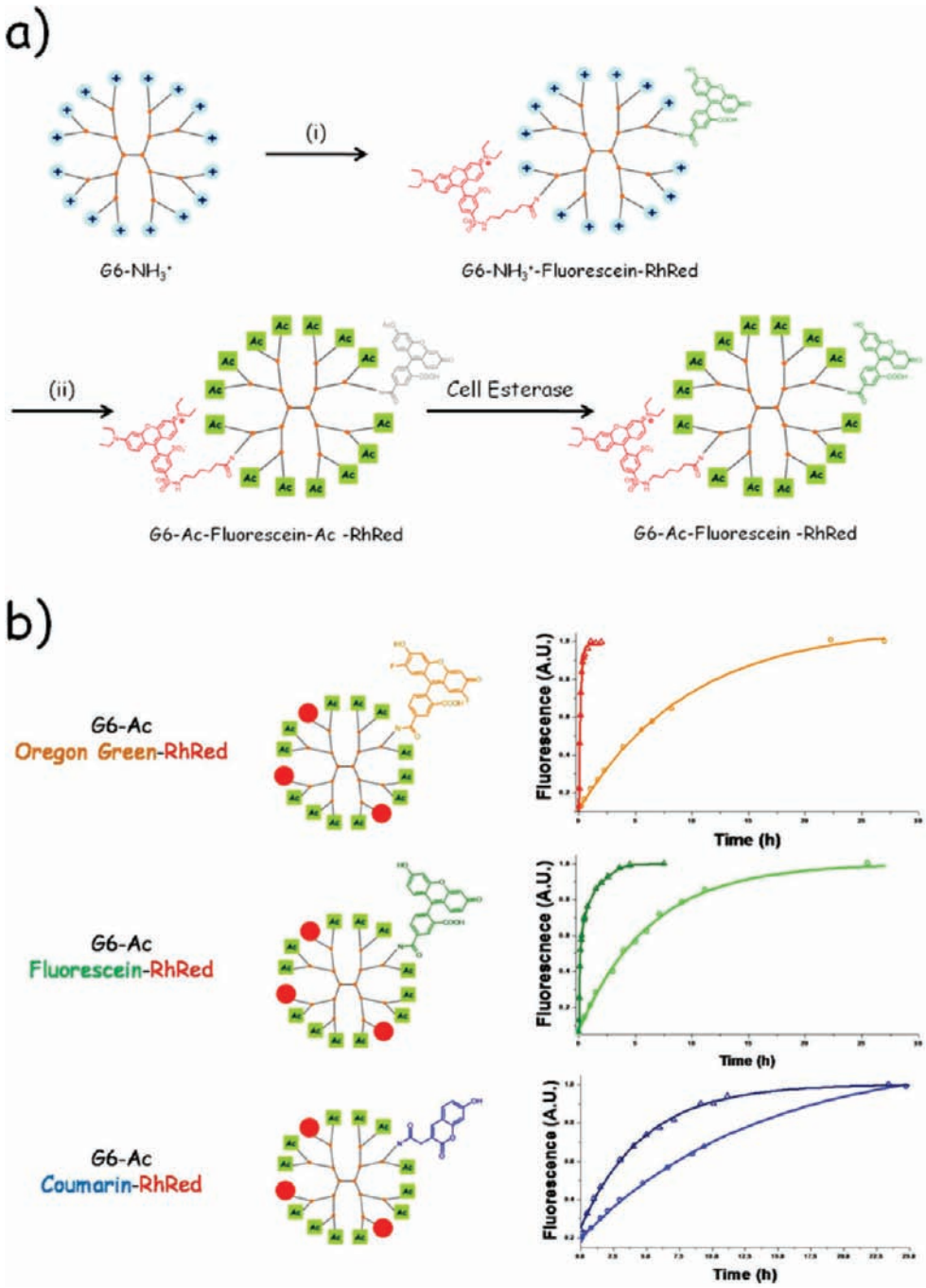

Figure 3. (a) Schematic procedure for preparation of dendrimer-based pH-sensors: (i) NHS-activated dyes, (ii) acetic anhydryde, triethylamine. (b) Hydrolysis kinetic studies for three different pH biosensors. Fluorescence recovery after acetylation was studied in PBS/lysis buffer (light-colored curves) in comparison with PBS/lysis buffer containing cytoplasmatic protein extract (dark-colored curves).

using ionophores. As shown in Figure 5a the sensor responds to pH changes with a variation of the green/red ratio (represented with a pseudocolor table). Note that as expected the concentration of the sensor is significantly different between the nucleus and the cytoplasm but the signal ratio is equal in the two compartments owing to the ratiometric correction. These measurements yielded the calibration curve shown in Figure 5b and show that care must be taken in transferring in vitro calibration curves to the cellular environment. Indeed the latter modifies the sensing properties of the dyes so that an intracellular calibration must be performed as shown here. On the basis of this procedure, we measured a pH value of 7.4 $\pm$ 0.1 in untreated cells. Also in this case some vesicular localization is observed and the ratiometric imaging demonstrates an acidic pH in these structures suggesting they are degradative organelles.

To exploit the dendrimer targeting ability described in the previous sections we electroporated into HeLa cells a cationic-G6 based pH sensor. As previously described, this dendritic structure labels the inner leaflet of the plasma membrane and lysosomes. Since the expected pH value is rather different in these two structures (acidic for the lysosome, neutral for the plasma membrane), this represents a useful test to demonstrate the ability of dendrimer-based sensor to achieve specific and localized ion-concentration measurements. Figure 6 shows the two channels and the ratio map for G6-Fluo-RhRed sensor.

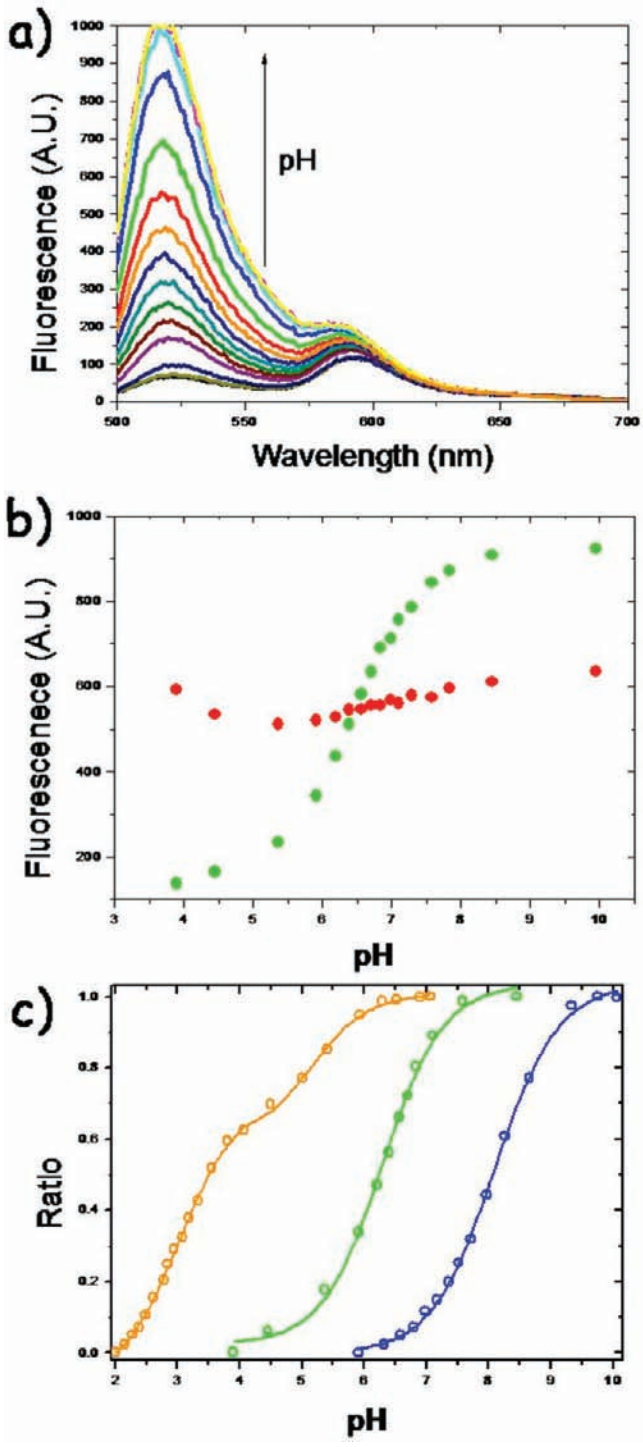

Figure 4. (a) Fluorescence emission spectra at different pH of Fluorescein inside G6-Ac-Fluo-RhRed sensor. (b) Green and red channel emissions of G6-Ac-Fluo-RhRed versus pH. (c) Fluorescence ratio at different pH for G6-Ac-Coumarin-RhRed (blue), G6-Ac-Fluorescein-RhRed (green), and G6-Ac-Oregon Green-RhRed.

As clearly shown by the pseudocolor map the green-to-red ratio is much different between the two organelles reflecting the expected large differences in pH, neutral for the membrane and strongly acidic for the lysosome. Notably none of the sensors have a dynamic range large enough to measure both the very low endosomal and the neutral cytosolic pH; indeed this analysis was intended to be qualitative to demonstrate the ability of this family of sensors to report differences in H^+ ion concentration in targeted compartments.

Discussion

Fluorescence biosensors are very powerful tools to unveil the role and the dynamics of ions and biomolecules in biological processes. Both GFPs and sensing organic dyes were successfully used for these purposes in vitro,[33] in living cells[11,20,34] and in vivo.[35] In particular, organic fluorophores were used to detect dynamic changes of a large number of analytes but suffer from several limitations such as difficult intracellular targeting, inability to perform ratiometric (and thus quantitative) measurements, and cell leakage.[21]

In this work, we demonstrate the use of dendrimer-based fluorescent biosensors to overcome some of the more severe limitations of organic dyes previously discussed. In fact, thanks to their multifunctionality, dendrimers act as scaffolds able to carry sensing fluorophores together with other analyte-insensitive dyes and therefore make it possible to perform ratiometric imaging. Recently Verkman and co-workers used dextran as scaffold for a ratiometric indicator for extracellular K^+.[14] PAMAM dendrimers, however, offer many advantageous chemical properties such us monodispersity, tunability of the physicochemical properties, and a very high chemical versatility of the surface groups. We took advantage of these features to tune dendrimer interactions in living cells and thus obtain intracellular targeting of the macromolecules.

We also showed a novel methodology for the cytoplasmic delivery of dendritic scaffolds by electroporation. This technique is routinely used for the transfection of GFP-based sensor and was also recently proposed for quantum dots.[36] In this way, we delivered fluorescent dendrimers directly into cells and could study by confocal microscopy the dynamics of these molecules inside living HeLa cells. This technique offers some interesting features such as (i) fast and effective delivery; (ii) direct delivery into the cytoplasm avoiding the complexity of endocytotic pathways;[23,37] (iii) delivery in parallel to the whole cell population. These characteristics make electroporation quite advantageous in comparison with other delivery techniques such as microinjection, direct incubation and liposome-based transfection.

Dendrimers varying in size (from G2 up to G6) and charge (cationic and neutral) were studied and revealed peculiar intracellular localizations. In particular cationic macromolecules display selective localization in nucleoli, plasma membrane and lysosomes probably owing to interactions with anionic macromolecules such as nucleic acids and membrane phospholipids.[28,38]

Neutral dendrimers on the contrary do not show any specific binding but undergo a nucleus-cytoplasm repartition according to dendrimer size; G6 PAMAMs are mainly localized in the cytoplasm since their size approaches the limit set by nuclear pores. Intracellular targeting is of much interest for biosensing, and it was obtained here by modulating the physicochemical

(33) Plafker, K.; Macara, I. G. *J. Biol. Chem.* **2002**, *277*, 30121–7.
(34) Emptage, N.; Bliss, T. V.; Fine, A. *Neuron* **1999**, *22*, 115–24.
(35) (a) Garaschuk, O.; Griesbeck, O.; Konnerth, A. *Cell Calcium* **2007**, *42*, 351–61. (b) Grewe, B. F.; Helmchen, F. *Curr. Opin. Neurobiol.* **2009**, *19*, 520–9.
(36) Derfus, A. M.; Chan, W. C.; Bhatia, S. N. *Adv. Mater.* **2004**, *16*, 961–966.
(37) Perumal, O. P.; Inapagolla, R.; Kannan, S.; Kannan, R. M. *Biomaterials* **2008**, *29*, 3469–76.
(38) Manunta, M.; Tan, P. H.; Sagoo, P.; Kashefi, K.; George, A. J. *Nucleic Acids Res.* **2004**, *32*, 2730–9.

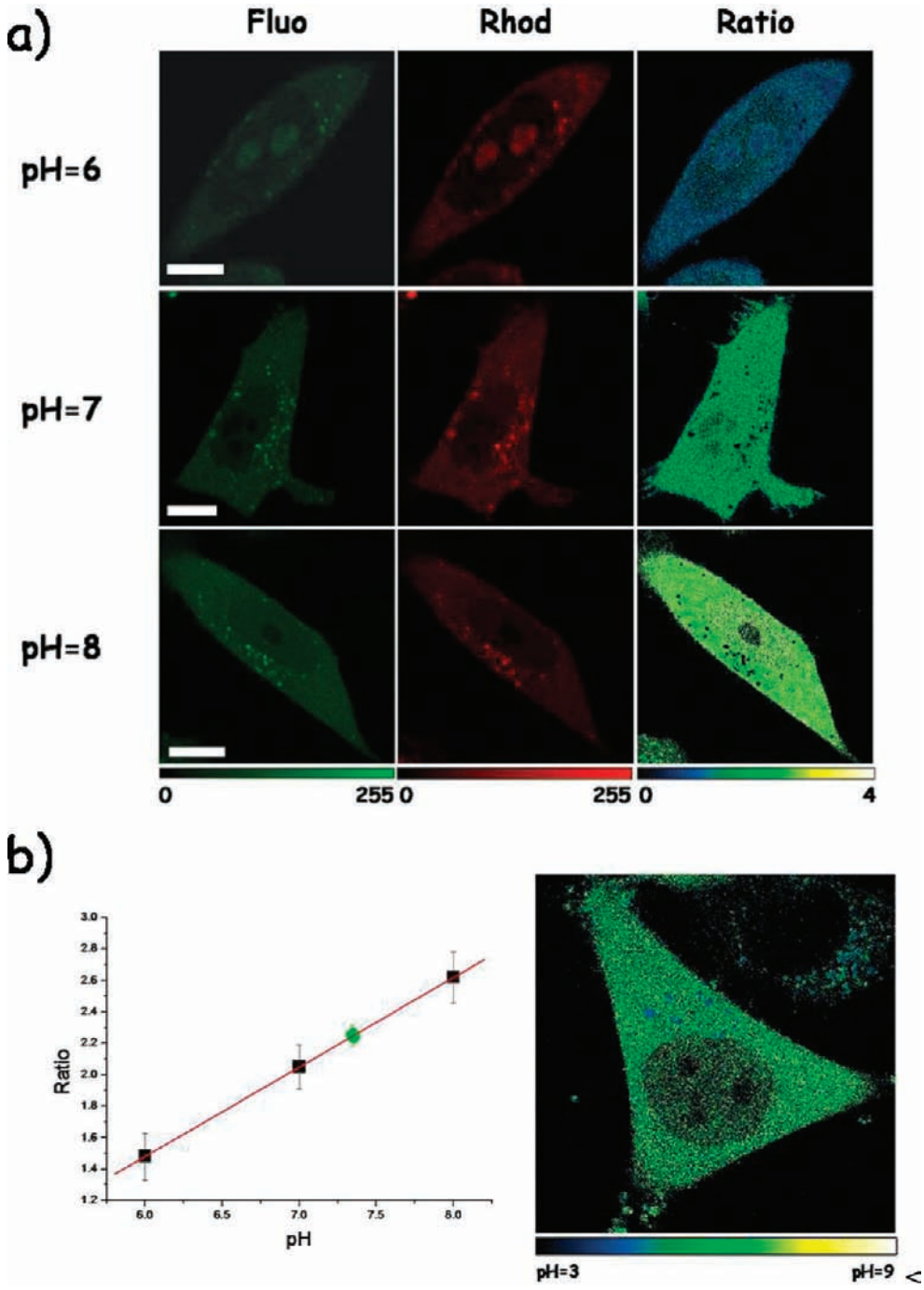

Figure 5. (a) Titration of G6-Ac-Fluo-RhRed in living cells. HeLa cells were clamped at pH = 6, pH = 7, and pH = 8 with H+ ionophores. (b) pH map (right) calculation for untreated HeLa cells based on the calibration curve obtained using ionophores (left). An average pH = 7.4 ± 0.1 was obtained. Scale bar = 15 μm.

properties of the dendrimer. This approach can be further extended by conjugating appropriate ligands or peptides to the scaffold to achieve targeting to a wider range of organelles. Interestingly, the localization of the neutral-G4 dendrimer is pH dependent. This can be related to the change of charge and structure of the inner part of the dendrimer at acidic pH.[32] This pH-triggered structural change deserves further study and could be exploited for the development of stimuli-responsive materials.

We synthesized ratiometric pH sensors by the conjugation of a pH-sensitive fluorophore together with an insensitive rhodamine. This modular approach was applied to three different sensor implementations tuned for H^+ affinity by replacing the sensing fluorophore. In this respect, the biosensors reported in this work should be regarded as a model for a whole family of dendrimer-based indicators. The same approach can be used to investigate a very large array of analytes simply by introducing the desired sensing dye.

We also showed that our procedure for dendrimer charged-amine acetylation leads to reversible fluorescence quenching, owing to the acetylation of the hydroxyl groups of the dyes; a hydrolysis kinetic study demonstrated a fast fluorescence recovery (time-scale of minutes) only in the presence of cytoplasmic enzymatic activity. This leads to the biosensor being

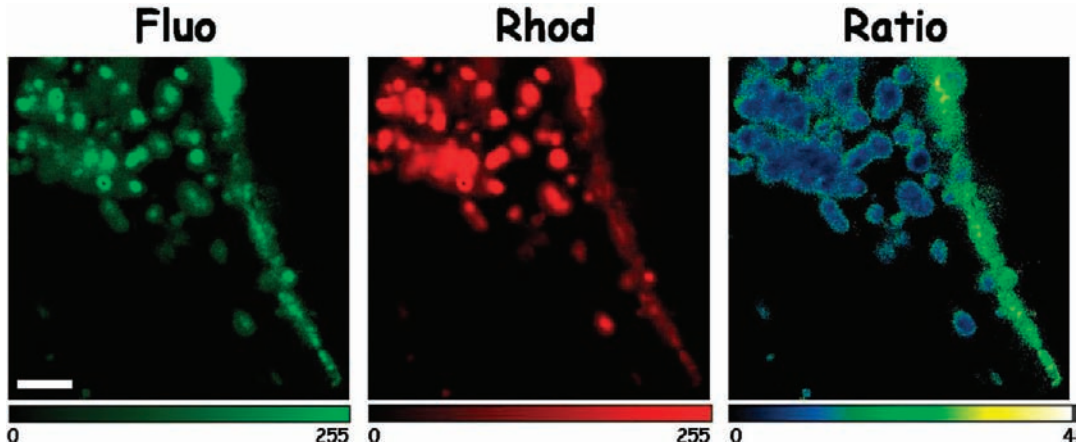

Figure 6. Targeted ratiometric pH imaging in plasma membrane and lysosomes with G6-NH_3^+-Fluo-RhRed. Dendrimer-based sensor specifically targets organelles owing to its surface cationic charge. Scale Bar = 5 μm.

active only inside cells and resembles the acetoxymethylester (AM ester) system that was successfully applied in many in vivo measurements.[39] Sensors were calibrated in vitro and the results are reported in Figure 4. As expected, the sensing dye shows a large change in fluorescence intensity upon pH titration, while the rhodamine signal is virtually unchanged (Figure 4b). The green-to-red ratios relative to the three biosensors were reported (Figure 4c) and demonstrate the ability to measure pH in different ranges (alkaline, near-neutral, and acidic for Coumarin, Fluorescein, and Oregon Green, respectively). Note that not all fluorophores retain their photophysical behavior upon dendrimer conjugation. This is particularly evident in the titration of Oregon Green that significantly deviates from the curve of the isolated fluorophore. Other fluorophores display changes of their fluorescence properties upon conjugation (data not shown) and this feature is currently under investigation. This does not hinder the successful applicability of the sensors presented in this work, but we believe that a thorough understanding of the fluorescent-dendrimer photophysics will allow the design of improved sensors.

After the in vitro study, we investigated the ability of the sensor to effectively indicate pH in living cells. For this purpose, the fluorescein-based sensor (based on an acetylated G6 dendrimer) was electroporated into HeLa cells in light of its ability to measure pH in the near-physiological range. As expected, the sensor retains the localization of the G6-Ac dendrimer; the cytoplasm and the nucleus of the cell are labeled albeit with a lower fluorescence signal from the latter. Signal was recorded in both green and red channels and a ratio image, obtained by dividing these two images pixel-by-pixel, was created. To calibrate the sensor, we clamped cell pH with ionophores and, as showed in Figure 5, a sizable increase in the green-to-red ratio was observed with alcalinization. From these ratio values a calibration curve was obtained, and an average cytoplasmatic value of pH = 7.4 $\pm$ 0.1 for untreated cells was measured. This value is consistent with previous reported measurements in cell lines and demonstrates the accuracy of the sensor.[11,40] Notably, despite the significant difference in sensor concentration between nucleus and cytoplasm the measured pH values in the two compartments coincide, indicating that the ratiometric correction successfully eliminates any influence of sensor concentration; this ability is of great importance for the in vivo application of the sensor where large concentration gradients in the samples can be expected but must not influence the pH reading. Figure 5 also highlights that sensor response is not influenced by its localization in a specific cell compartment; in fact, the signal ratio is constant between different organelles (nucleus, nucleoli, and cytoplasm). The stability of sensor response in different environments was further demonstrated by pH measurements in another cell line (CHO cells), providing comparable results (see Supporting Information).

Our approach can benefit from the high sensitivity of fluorescence-related techniques. Two main aspects had to be considered to achieve a good signal allowing a high signal-to-noise measurement: the dendrimer intracellular concentration and the brightness of the sensors. Dendrimer intracellular concentration is related (but not equal) to the concentration in the outside medium during electroporation and should be as low as possible to avoid an influence of the probe on intracellular pH homeostasis. As shown in the Supporting Information the concentration used in this study does not influence cell pH as cells with different sensor concentration display the same green-to-red ratio and thus the same pH. Sensor brightness can be enhanced by the conjugation of multiple dyes on the dendrimer scaffold taking advantage of its multifunctionality. However, photophysical phenomena, for example, quenching and excimer formation, occurring when multiple dyes are confined close together do have to be taken in account. Several aspects of photophysical properties of dye dendrimer conjugates are currently under investigation.

Finally, we exploited the targeting ability of G6 cationic dendrimers to realize a localized pH imaging in lysosomes and plasma membranes. This situation is particularly suitable to test the performance of the sensor since these two subcellular structures have different pH: acidic for lysosome and neutral for plasma membrane. Figure 6 shows that the sensor does highlight the pH differences with a marked change in the green-to-red ratio. Notably the sensor is able to detect the acidic pH also for lysosomal vesicles close to the plasma membrane thanks to the available confocal-microscope resolution.

Our work tries to develop a new approach in intracellular ion sensing. Other methodologies have already been proposed using fluorescent dyes, fluorescent proteins, and fluorescent nanoparticles.[17] Starting from the promising results obtained with fluorescent organic dyes in pH sensing, we tried to

(39) Haworth, R. A.; Redon, D. *Cell Calcium* **1998**, *24*, 263–73.
(40) Arosio, D.; Ricci, F.; Marchetti, L.; Gualdani, R.; Albertazzi, L.; Beltram, F. *Nat. Methods* **2010**, *7*, 516–518.

overcome some of their limitations (difficulties in targeting, impossibility to achieve ratiometric imaging, cell leakage, low brightness) exploiting the conjugation to a macromolecular scaffold able to vehiculate multiple functional dyes. Some disadvantages of our approach in comparison with the use of organic dyes (often commercially available and membrane permeable) can be found in the synthetic efforts needed for the biosensor synthesis and the more complicated delivery method. However the proposed approach seems very promising thanks to its improved properties; importantly its modularity allows us to define a new family of biosensors for the investigation of a number of biological processes.

Acknowledgment. Useful discussions with Dr. Ranieri Bizzarri are gratefully acknowledged. We thank Dr. Emilia Bramanti for her precious help with FT-IT measurements. This work was partially supported by the Italian Ministry for University and Research (MiUR) under the framework of FIRB project RBLA03ER38.

Supporting Information Available: Supporting figures are available online. This material is available free of charge via the Internet at http://pubs.acs.org.

JA105689U